A&A 400, 695–707 (2003)
DOI: 10.1051/0004-6361:20021790

Astronomy & Astrophysics

ISO-SWS calibration and the accurate modelling of cool-star atmospheres⋆,⋆⋆

III. A0 to G2 stars

L. Decin[1,⋆⋆⋆], B. Vandenbussche[1], C. Waelkens[1] K. Eriksson[2], B. Gustafsson[2], B. Plez[3], and A. J. Sauval[4]

[1] Instituut voor Sterrenkunde, KULeuven, Celestijnenlaan 200B, 3001 Leuven, Belgium
[2] Institute for Astronomy and Space Physics, Box 515, 75120 Uppsala, Sweden
[3] GRAAL - CC72, Université de Montpellier II, 34095 Montpellier Cedex 5, France
[4] Observatoire Royal de Belgique, Avenue Circulaire 3, 1180 Bruxelles, Belgium

Received 22 November 2001 / Accepted 2 December 2002

Abstract. Vega, Sirius, β Leo, α Car and α Cen A belong to a sample of twenty stellar sources used for the calibration of the detectors of the Short-Wavelength Spectrometer on board the Infrared Space Observatory (ISO-SWS). While general problems with the calibration and with the theoretical modelling of these stars are reported in Decin et al. (2003), each of these stars is discussed individually in this paper. As demonstrated in Decin et al. (2003), it is not possible to deduce the effective temperature, the gravity and the chemical composition from the ISO-SWS spectra of these stars. But since ISO-SWS is absolutely calibrated, the angular diameter (θ_d) of these stellar sources can be deduced from their ISO-SWS spectra, which consequently yields the stellar radius (R), the gravity-inferred mass (M_g) and the luminosity (L) for these stars. For Vega, we obtained $\theta_d = 3.35 \pm 0.20$ mas, $R = 2.79 \pm 0.17\,R_\odot$, $M_g = 2.54 \pm 1.21\,M_\odot$ and $L = 61 \pm 9\,L_\odot$; for Sirius $\theta_d = 6.17 \pm 0.38$ mas, $R = 1.75 \pm 0.11\,R_\odot$, $M_g = 2.22 \pm 1.06\,M_\odot$ and $L = 29 \pm 6\,L_\odot$; for β Leo $\theta_d = 1.47 \pm 0.09$ mas, $R = 1.75 \pm 0.11\,R_\odot$, $M_g = 1.78 \pm 0.46\,M_\odot$ and $L = 15 \pm 2\,L_\odot$; for α Car $\theta_d = 7.22 \pm 0.42$ mas, $R = 74.39 \pm 5.76\,R_\odot$, $M_g = 12.80^{+24.95}_{-6.35}\,M_\odot$ and $L = 14573 \pm 2268\,L_\odot$ and for α Cen A $\theta_d = 8.80 \pm 0.51$ mas, $R = 1.27 \pm 0.08\,R_\odot$, $M_g = 1.35 \pm 0.22\,M_\odot$ and $L = 1.7 \pm 0.2\,L_\odot$. These deduced parameters are confronted with other published values and the goodness-of-fit between observed ISO-SWS data and the corresponding synthetic spectrum is discussed.

Key words. infrared: stars – stars: atmospheres – stars: fundamental parameters

1. Introduction

In the first two papers of this series (Decin et al. 2000; Decin et al. 2003, hereafter referred to as Paper I and Paper II respectively), a method is described to analyse a sample of ISO-SWS spectra of standard stars in a consistent way. We did not only concentrate on the possibility to extract reliable stellar parameters from the medium-resolution ISO-SWS spectra, but have also demonstrated where problems in the computation of synthetic spectra – based on the MARCS and TURBOSPECTRUM code (Gustafsson et al. 1975; Plez et al. 1992, 1993, version May 1998 – and in the calibration of the ISO-SWS detectors destroy the goodness-of-fit between observed and synthetic spectra (Paper II). These general results were based on a sample of 5 warm ($T_{\rm eff} > T_{\rm eff,\odot}$) and 11 cool stars. In this paper, we will further analyse these 5 warm stars – α Cen A, β Leo, α Car, Sirius and Vega – in order to extract relevant astrophysical data.

After a description of the general problems for these warm stars in Sect. 2 (as described in Paper II), we will outline the method of analysis to deduce different stellar parameters in Sect. 3 (based on the results of Papers I and II). In the different subsections of Sect. 3, each star will be discussed individually. In order to assess the observed accuracy, some specific calibration details will be given. If available, different AOT01 observations[1] (i.e. a full SWS scan at reduced spectral resolution, with four possible scan speeds) are compared with each other to demonstrate the calibration precision of ISO-SWS. With these

Send offprint requests to: L. Decin,
e-mail: `Leen.Decin@ster.kuleuven.ac.be`

⋆ Based on observations with ISO, an ESA project with instruments funded by ESA Member States (especially the PI countries France, Germany, The Netherlands and the UK) and with the participation of ISAS and NASA.

⋆⋆ Appendices A and B are only available in electronic form at `http://www.edpsciences.org`

⋆⋆⋆ *Postdoctoral Fellow of the Fund for Scientific Research, Flanders.*

[1] Each observation is determined uniquely by its observation number (8 digits), in which the first three digits represent the revolution number. The observing data can be calculated from the revolution number which is the number of days after 17 November 1995.

remarks in mind, the synthetic spectrum based on assumed and deduced parameters is confronted with the ISO-SWS spectrum. Furthermore, we will discuss why we have assumed certain parameters and we will confront the deduced parameters from the ISO-SWS spectra with other literature values.

The appendix of this article is published electronically. Most of the grey-scale plots in the printed version of the article are printed in colour in the appendix, in order to better distinguish the different spectra.

2. Summary of general discrepancies (Paper II)

For the warm stars in our sample, the origin of the general discrepancies between the ISO-SWS and synthetic spectra could be reduced to 1. inaccurate atomic oscillator strengths in the infrared, 2. problematic computation of hydrogenic line broadening, 3. fringes at the end of band 1D (3.02–3.52 μm), 4. inaccurate Relative Spectral Response Function (RSRF) at the beginning of band 1A (2.38–2.60 μm) and 5. memory effects in band 2 (4.08–12.00 μm).

3. Stellar parameters

In Paper I of this series, a method was described to determine stellar parameters from the band-1 data (2.38–4.08 μm) of ISO-SWS spectra. This method was based on the presence of different molecular absorbers in this wavelength range, each having their own characteristic absorption pattern. Since the infrared absorption pattern of these A0–G2 stars is completely dominated by atoms (with the exception of α Cen A, for which the CO first overtone and fundamental bands are weakly visible) this method of analysis could not be applied to these stars. Moreover, it was demonstrated in Paper II that there are still quite some problems with the oscillator strengths of infrared atomic transitions. It was therefore impossible to determine the effective temperature ($T_{\rm eff}$), the gravity ($\log g$), the microturbulence (ξ_t), the metallicity ([Fe/H]) and the abundance of carbon, nitrogen and oxygen for these warm stars from their ISO-SWS spectra. In order to further analyse these spectra, we have performed a detailed literature study to find accurate values for these stellar parameters. Using these parameter values, synthetic spectra were computed for each target. From the absolutely calibrated ISO-SWS spectra, we then could deduce the angular diameter (θ_d). The angular diameter together with the Hipparcos' parallax (with the only exception of α Cen A for which a more precise parallax by Pourbaix et al. (1999) is available) then yielded the stellar radius. Together with the assumed gravity and effective temperature, the gravity-inferred mass (M_g) and the stellar luminosity (L) are derived.

The resultant stellar parameters are summarised in Table 1. The objects have been sorted by spectral type. Since the error bars of certain assumed stellar parameters were necessary for the propagation to the mean error of other deduced parameters (see Eq. (18) in Paper I), the error bars on all stellar parameters are given. The mean error on the angular diameter is estimated from the intrinsic error, the absolute flux error (10%) and the error in the assumed effective temperature (see Paper II). Whenever $\sigma(\log g) \geq 0.40$, the lower and upper limit of the gravity-inferred mass M_g are estimated as being 2/3 of the *maximum* error. In the subsequent subsections, each star will be discussed individually. A short description of the methods and/or data used and on the parameters assumed and deduced by the different authors quoted in next sections, can be found in the electronic version of the appendix.

3.1. α Cen A: AOT01, speed 4, revolution 607

3.1.1. Some specific calibration details

Since α Cen A is component of a binary, one has to check the flux contribution of the second component (HIC 71681, K1 V). From the coordinates of the system in 1997, its proper motion and the correction for the orbit, one obtains

$$\begin{cases} \alpha_A = 14\text{h } 39\text{m } 24.13\text{s} \\ \delta_A = -60\text{deg } 49' \, 17.9'' \end{cases}$$

$$\begin{cases} \alpha_B = 14\text{h } 39\text{m } 22.73\text{s} \\ \delta_B = -60\text{deg } 49' \, 30.4''. \end{cases}$$

This results in a difference in spacecraft coordinates of $dy = -12.1241''$ and $dz = 10.9342''$. Taking the pointing jitter into account ($\leq 1.5''$), and the fact that the average difference between the G and K star in the wavelength range from 1.6 μm to 11.2 μm is $0.91^{\rm m}$ (Cohen et al. 1996a), one can calculate that the maximal flux contribution from the K dwarf around 3 μm is 6 Jy, which is negligible.

The factors, by which the data of the different sub-bands are multiplied (see Table 3 in Paper II) show a good agreement with the band-border ratios determined by Feuchtgruber (1998). The only exception is band 2C, but this is not so significant, due to the large scatter for the band-border ratio between band 2B and band 2C (Fig. 6 in Feuchtgruber 1998) and the memory effects in band 2.

3.1.2. Comparison with other AOT01 observations

Alpha Cen A has also been observed during revolution 294 with the AOT01 speed-1 option. The pointing offsets were $dy = -0.797''$ and $dz = -0.832''$. Also for this observation, the contribution of the K main-sequence companion of α Cen A is negligible. The data of both band 1B and band 1E have been multiplied by a factor 1.01. The relative features match quite well taking the uncertainties of the speed-1 observation into account. There is, however, a difference in absolute flux level of 16% (Fig. 1). In revolution 294, the activation of the scientific measurements was started later than usual because of the time allocated for the Delta-V manoeuvre and the measurement of the superfluid He mass. These two activities may have influenced the quality of the speed-1 observation. As will be argued in a subsequent article in this series – where we will confront the obtained synthetic spectra with the templates of Cohen (Cohen et al. 1992b, 1995, 1996b; Witteborn et al. 1999) – it is reasonable to assume that the absolute flux level of the speed-4 observation is somewhat too high. Since the absolute flux accuracy is quoted to be ~10%, this 16% flux-difference is still within the quoted error bar.

Table 1. Fundamental stellar parameters for the selected stars in the sample. The effective temperature $T_{\rm eff}$ is given in K, the logarithm of the gravity in cgs units, the microturbulent velocity ξ_t in km s^{-1}, the angular diameter in mas, the parallax π in mas, the distance D in parsec, the radius R in $R_\odot$, the gravity-inferred mass M_g in $M_\odot$ and the luminosity L in $L_\odot$.

	α Lyr	α CMa	β Leo	α Car	α Cen A
Sp. Type	A0 V	A1 V	A3 Vv	F0 II	G2 V
$T_{\rm eff}$	9650 ± 200	10150 ± 400	8630 ± 200	7350 ± 300	5830 ± 30
$\log g$	3.95 ± 0.20	4.30 ± 0.20	4.20 ± 0.10	1.80 ± 0.50	4.35 ± 0.05
ξ_t	2.0 ± 0.5	2.0 ± 0.5	2.0	3.25 ± 0.25	1.0 ± 0.1
[Fe/H]	−0.40 ± 0.30	0.50 ± 0.30	0.20	−0.24 ± 0.04	0.25 ± 0.02
ε(C)	8.42 ± 0.15	7.97 ± 0.15	8.76	8.41 ± 0.10	8.74 ± 0.05
ε(N)	8.00 ± 0.15	8.15 ± 0.15	8.25	8.68 ± 0.05	8.26 ± 0.09
ε(O)	8.74 ± 0.15	8.55 ± 0.12	9.13	8.91 ± 0.10	9.13 ± 0.06
θ_d	3.35 ± 0.20	6.17 ± 0.38	1.47 ± 0.09	7.22 ± 0.42	8.80 ± 0.51
π	128.93 ± 0.55	379.21 ± 1.58	90.16 ± 0.89	10.43 ± 0.53	737.0 ± 2.6
D	7.76 ± 0.03	2.63 ± 0.01	11.09 ± 0.11	95.88 ± 4.87	1.36 ± 0.01
R	2.79 ± 0.17	1.75 ± 0.11	1.75 ± 0.11	74.39 ± 5.76	1.27 ± 0.08
M_g	2.54 ± 1.21	2.22 ± 1.06	1.78 ± 0.46	$12.77^{+24.95}_{-6.35}$	1.35 ± 0.22
L	61 ± 9	29 ± 6	15 ± 2	14573 ± 2268	1.7 ± 0.2

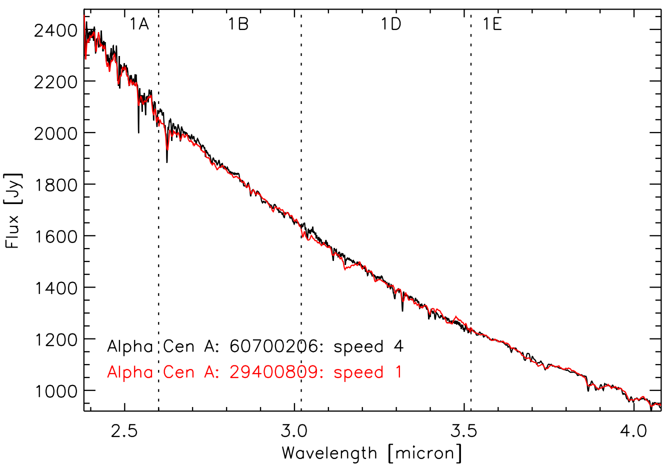

Fig. 1. Comparison between the AOT01 speed-4 observation of α Cen A (revolution 607) and the speed-1 observation (revolution 294). The data of the speed-1 observation have been multiplied by a factor 1.16. A coloured version of this plot is available in the appendix as Fig. A.1.

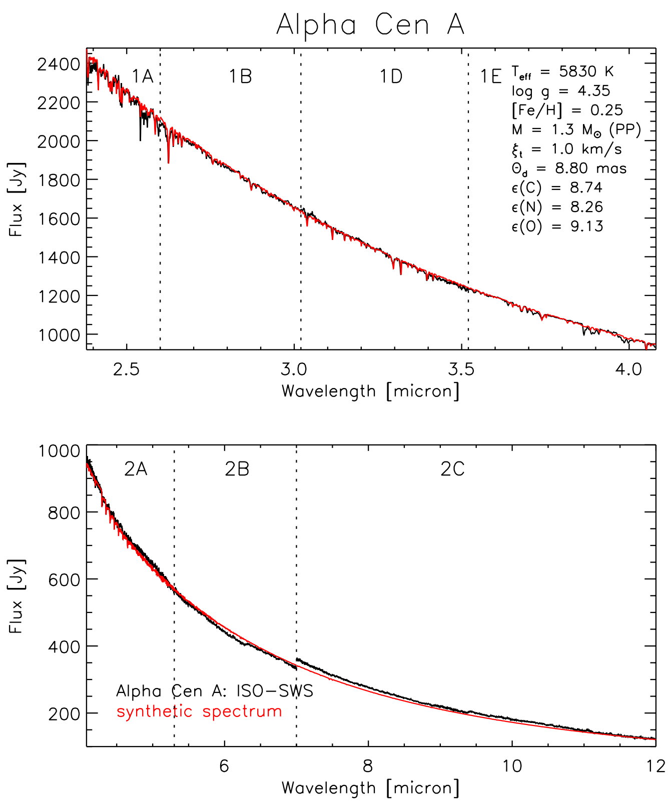

Fig. 2. Comparison between band 1 and band 2 of the ISO-SWS data of α Cen A (black) and the synthetic spectrum (grey) with stellar parameters $T_{\rm eff}$ = 5830 K, $\log g$ = 4.35, M = 1.3 $M_\odot$, [Fe/H] = 0.25, ξ_t = 1.0 km s^{-1}, ε(C) = 8.74, ε(N) = 8.26, ε(O) = 9.13 and θ_d = 8.80 mas. A coloured version of this plot is available in the appendix as Fig. A.2.

3.1.3. Comparison between the ISO-SWS spectrum and the synthetic spectrum (Fig. 2)

As discussed in Paper II, it is quite difficult to pin down the fundamental parameters of α Cen A from the SWS-spectrum, due to the absence of molecular features. Therefore, the parameters found by Neuforge-Verheecke & Magain (1997) were used to calculate the corresponding synthetic spectrum. Subsequently, the angular diameter, radius, mass and luminosity were derived. This resulted in the following parameters: $T_{\rm eff}$ = 5830 ± 30 K, $\log g$ = 4.35 ± 0.05, ξ_t = 1.0 ± 0.1 km s^{-1}, [Fe/H] = 0.25 ± 0.02, ε(C) = 8.74 ± 0.05, ε(N) = 8.26 ± 0.09, ε(O) = 9.13 ± 0.06, π = 737.0 ± 2.6 mas, θ_d = 8.80 ± 0.51 mas, R = 1.27 ± 0.08 $R_\odot$, M_g = 1.35 ± 0.22 $M_\odot$ and L = 1.7 ± 0.2 $L_\odot$, with deviation estimating parameters from the Kolmogorov-Smirnov test (see Paper I) being β_{1A} = 0.043, β_{1B} = 0.036, β_{1D} = 0.063, β_{1E} = 0.024.

Looking to the relative contribution of the different chemical species (see Fig. 3.1 in Decin 2000) and to the Atmospheric

Trace Molecule Spectroscopy (ATMOS) spectrum of the Sun (Geller 1992; Gunson et al. 1996), it is obvious that the atoms dominate the infrared spectrum of α Cen A, although the CO fundamental and first-overtone bands start arising around 4.4 μm and 2.4 μm respectively. As described in Paper II, problems with inaccurate oscillator strengths of the atomic lines in the infrared in the line list of Hirata & Horaguchi (1995) caused quite some discrepancies between the ISO-SWS and synthetic spectra. By using the identifications given by Geller (1992) for the ATMOS solar spectrum, the strongest contributors to the most prominent features were identified, with the strongest lines originating from Fe, Al, Si and Mg transitions (see, e.g., Fig. 5 in Paper II). The largest difference between the ISO-SWS spectrum of α Cen A and the rebinned ATMOS spectrum of the Sun occurs around 2.4 μm. As discussed in Paper II, the origin of this problem is situated in the problematic RSRF of band 1A in this wavelength region. The problems with the computation of the Humphreys lines near the Humphreys ionisation edge result in $\beta_{\rm 1D}$ being higher than the maximum acceptable value for this sub-band as given in Table 3 in Paper I.

3.1.4. Comparison with other published stellar parameters

– Assumed parameters:
  It has to be noted that the fundamental stellar parameters ($T_{\rm eff}$, $\log g$, $\xi_{\rm t}$, [Fe/H], ε(C), ε(N), ε(O)), determined by several authors using different methods, are in excellent agreement (see Table 2). Since the most up-to-date spectroscopic analysis based on high-resolution and high signal-to-noise spectra of α Cen A was performed by Neuforge-Verheecke & Magain (1997), their derived parameters were used as input parameters.
– Deduced parameters:
  The angular diameter deduced from the AOT01 speed-4 observation of α Cen A (revolution 607), is somewhat larger than the values obtained by other indirect methods, but is still within the error bars of the other values. The origin of the difference may be too high a flux level of the ISO-SWS AOT01 speed-4 observation (see Sect. 3.1.2). As a consequence, the stellar radius, gravity-inferred mass and luminosity are also somewhat larger than the other values listed in Table 2. Different methods were used by different authors to estimate the radius of α Cen A: using $T_{\rm eff}$ and L (e.g., Soderblom 1986; Furenlid & Meylan 1990), using $\theta_{\rm d}$ and π (e.g., Volk & Cohen 1989) or using the p-mode oscillations found in α Cen A (e.g., Pottasch et al. 1992). The same can be said for the luminosity, where Flannery & Ayres (1978) have used different broad-band systems and narrow-band photometric indices to estimate the luminosity; Volk & Cohen (1989) and Pottasch et al. (1992) have used the assumed $T_{\rm eff}$ and deduced R-values. The most quoted mass value for α Cen A is the one deduced by Demarque et al. (1986) ($M = 1.085 \pm 0.010\,M_\odot$). Pourbaix et al. (1999) found for the first time an agreement between astrometric and spectroscopic mass ratio. Their value for the mass ($M = 1.160 \pm 0.031\ M_\odot$) is in better agreement with a mass estimated from the evolutionary tracks of Girardi et al. (2000) (for $T_{\rm eff} = 5830$ K and $L = 1.7\,L_\odot$, we found $M = 1.02 \pm 0.20\,M_\odot$) than our gravity-inferred mass of $1.30 \pm 0.21\,M_\odot$.

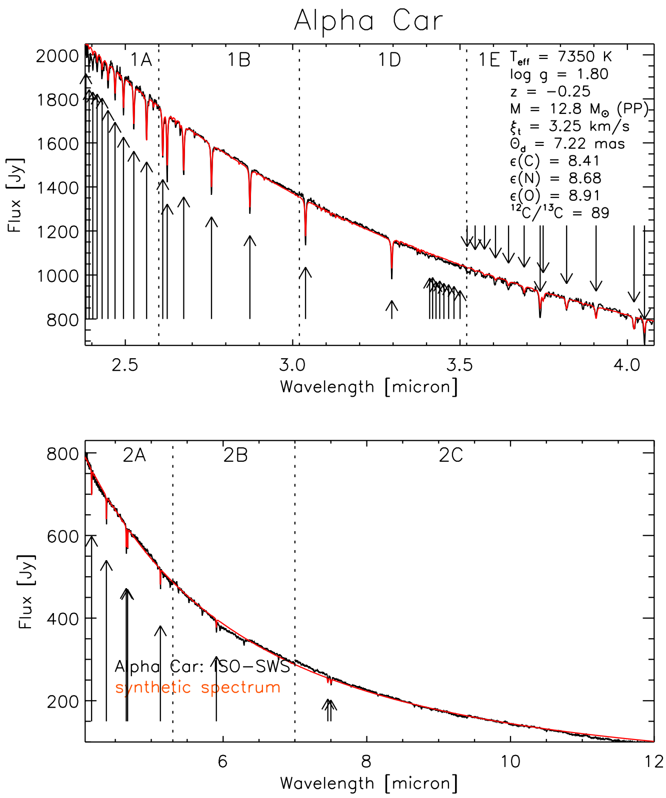

Fig. 3. Comparison between band 1 and band 2 of the ISO-SWS data of α Car (black) and the synthetic spectrum (grey) with stellar parameters $T_{\rm eff} = 7350$ K, $\log g = 1.80$, $M = 12.8\,M_\odot$, [Fe/H] $= -0.25$, $\xi_{\rm t} = 3.25$ km s^{-1}, ε(C) = 8.41, ε(N) = 8.68, ε(O) = 8.91 and $\theta_{\rm d} = 7.22$ mas. Hydrogen lines are indicated by arrows. A coloured version of this plot is available in the appendix as Fig. A.3.

3.2. α Car: AOT01, speed 4, revolution 729

3.2.1. Some specific calibration details

Only the band-1A flux had to be multiplied with a factor larger than 1.02, although this is still smaller than the mean band-border ratio between band 1A and band 1B for that revolution (see Fig. 1 in Feuchtgruber 1998).

3.2.2. Comparison between the ISO-SWS spectrum and the synthetic spectrum (Fig. 3)

Using the stellar parameters $T_{\rm eff} = 7350$ K, $\log g = 1.80$, $\xi_{\rm t} = 3.25$ km s^{-1}, [Fe/H] $= -0.24$, ε(C) = 8.41, ε(N) = 8.68, ε(O) = 8.91 (Desikachary & Hearnshaw 1982) and $\pi = 10.43 \pm 0.53$ mas results in $\theta_{\rm d} = 7.22 \pm 0.42$ mas, $R = 74.39 \pm 5.76\,R_\odot$, $M_{\rm g} = 12.80^{+24.95}_{-6.35}\,M_\odot$ and $L = 14\,573 \pm 2268\,L_\odot$ with deviation estimating parameters $\beta_{\rm 1A} = 0.091$, $\beta_{\rm 1B} = 0.045$, $\beta_{\rm 1D} = 0.091$, $\beta_{\rm 1E} = 0.041$.

Table 2. Literature study of α Cen A, with the effective temperature $T_{\rm eff}$ given in K, the mass M in $M_\odot$, the microturbulent velocity ξ_t in km s^{-1}, the angular diameter θ_d in mas, the luminosity L in $L_\odot$ and the radius R in $R_\odot$. Angular diameters deduced from direct measurements (e.g. from interferometry) are written in italic, while others (e.g. from spectrophotometric comparisons) are written upright. Assumed or adopted values are given between parentheses. The results of this research are mentioned in the last line. Only the error bars on the *deduced* parameters are given. A short description of the methods and/or data used by the several authors can be retrieved from `http://www.ster.kuleuven.ac.be/~leen/artikels/ISO3/appendix.ps`.

$T_{\rm eff}$	$\log g$	M	ξ_t	[Fe/H]	ε(C)	ε(N)	ε(O)	θ_d	L	R	Ref.
5800								8.62 ± 0.23			1.
5800 ± 100		1.11 ± 0.03							1.51 ± 0.06		2.
		1.10									3.
5750 ± 30	4.38 ± 0.07	1.08	1.0	0.28 ± 0.15							4.
		1.085 ± 0.010									5.
5820 ± 50	4.40 ± 0.05		1.54 ± 0.08	0.20 ± 0.04							6.
5770 ± 20										1.23	7.
(5770)	4.5		(1.0)	0.22 ± 0.15							8.
(5750)	4.42 ± 0.11		(1.5)	(0.28)							9.
5700 ± 75									1.446	1.23 ± 0.03	10.
5710 ± 25	4.27 ± 0.20	(1.085)	1.0 ± 0.2	0.12 ± 0.06	8.77 ± 0.04		8.98 ± 0.06			1.26	11.
5834 ± 140											12.
5800 ± 20	4.31 ± 0.02	(1.085)	(1.0)	0.22 ± 0.02							13.
5760								8.52			14.
5710		(1.085)							1.33 ± 0.11	1.17 ± 0.05	15.
	4.3	1.4									16.
(5770)	(4.29)		1.28 ± 0.05$\vert$1.17 ± 0.06	0.00							17.[a].
(5770)	(4.29)		1.48-1.06 $\vert$	0.30							17.[b].
5830 ± 30	4.34 ± 0.05	(1.085)	1.09 ± 0.11	0.25 ± 0.02	8.74 ± 0.05	8.26 ± 0.09	9.13 ± 0.06		1.5		18.
		1.160 ± 0.031									19.
(5830)	(4.35)	1.35 ± 0.22	(1.0)	(0.25)	(8.74)	(8.26)	(9.13)	8.80 ± 0.51	1.7 ± 0.2	1.27 ± 0.08	20.

1. Blackwell & Shallis (1977); 2. Flannery & Ayres (1978); 3. Kamper & Wesselink (1978); 4. England (1980); 5. Demarque et al. (1986); 6. Smith & Lambert (1986); 7. Soderblom (1986); 8. Abia et al. (1988); 9. Edvardsson (1988); 10. Volk & Cohen (1989); 11. Furenlid & Meylan (1990); 12. McWilliam (1990); 13. Chmielewski et al. (1992); 14. Engelke (1992); 15. Pottasch et al. (1992); 16. Popper (1993); 17. Gadun (1994); 18. Neuforge-Verheecke & Magain (1997); 19. Pourbaix et al. (1999); 20. present results.

Just as for α Cen A, the large β-values from the Kolmogorov-Smirnov test may be explained by the problematic prediction of the atomic lines and especially the hydrogen lines (which dominate the spectral signature) and the noise. The more pronounced discrepancy visible at the beginning of band 1A is due to calibration problems (RSRF). The lower gravity of α Car with respect to the other *warm* stars is reflected in the smaller broadening of the hydrogen lines. Despite this lower gravity, all but one sub-band are rejected by the Kolmogorov-Smirnov test.

3.2.3. Comparison with other published stellar parameters

– Assumed parameters:
From Table 3, it is clearly apparent that a gravity determined in a spectroscopic way (i.e. by requiring that the abundance of neutral and ionised lines yield the same abundance) is usually lower than a photometric gravity (i.e. determined from photometric colours, or by using the well-known relation between g, $T_{\rm eff}$, M and L, where the mass has been determined by locating the stellar object on theoretical evolutionary tracks). It is well known that the accuracy of spectroscopic determinations of gravities from ionisation equilibria or molecular equilibria for individual stars is not very good for giants (cf., e.g., Trimble & Bell 1981; Brown et al. 1983; Smith & Lambert 1985). Therefore, the values given by Desikachary & Hearnshaw (1982) were adopted as atmospheric parameters for α Car.

– Deduced parameters:
The angular diameter derived from the ISO-SWS data is larger than the two values based on the InfraRed Flux Method (IRFM, Blackwell & Shallis 1977; Blackwell et al. 1980) in Table 3. Napiwotzki et al. (1993) quoted that temperatures deduced by using the IRFM are *too low* by 1.6–2.8%, corresponding to angular diameters which are too large by 3.5–5.9%. When inspecting the other stars of the sample which have been analysed by means of the IRFM, this trend however is not visible. The reason for the discrepancy in angular diameter may be the problematic determination of the continuum in the spectrum of a *warm* star Paper II. This larger angular diameter however can not explain the difference in radius and luminosity seen between our results and other literature values. Lyubimkov & Boyarchuk (1984) have estimated a mass value of 8 ± 1.5 $M_\odot$ for α Car from the evolutionary tracks of Becker (1981) in the $\log T_{\rm eff}$–$\log g$ plane. Also Russell & Bessell (1989) have determined the mass from evolutionary tracks. Together with the gravity mentioned by Boyarchuk & Lyubimkov (1983), this results in the stellar radius of $\sim$53 $R_\odot$. Using $V - I = 0.44$ (Johnson et al. 1966), the bolometric correction BC_I from Bessell et al. (1998) and the Hipparcos' parallax, we obtain $M_{\rm bol} = -5.68 \pm 0.12$ (L = 14723 ± 1654 $L_\odot$), in agreement with our $T_{\rm eff}$ based luminosity. From the evolutionary tracks of Claret & Gimenez (1995) we estimate a somewhat higher mass value being 10.5 ± 0.5 $M_\odot$. When our gravity-inferred mass of 12.8 $M_\odot$ would have been used by Lyubimkov & Boyarchuk (1984) and Russell & Bessell (1989), a stellar radius of 67 $R_\odot$ and

Table 3. See caption of Table 2, but now for α Car.

$T_{\rm eff}$	$\log g$	M	ξ_t	[Fe/H]	ε(C)	ε(N)	ε(O)	θ_d	L	R	Ref.
								6.6 ± 0.8			1.
7460 ± 460								*(6.6)*			2.
7206 ± 173								7.08 ± 0.19			3.
7420											4.
7500 ± 200	1.85 ± 0.30		2.7 ± 1.0	0.35 ± 0.15							5.
7346 ± 150								6.81 ± 0.20			6.
7350 ± 300	1.80 ± 0.50		3.25 ± 0.25	−0.24 ± 0.04	8.41 ± 0.10	8.68 ± 0.05	8.91 ± 0.10				7.
7400 ± 150	1.9 ± 0.2		4.5|6.0								8.
(7400)	(1.9)	8 ± 1.5	(4.5)	−0.10	8.32				7500	53	9.
7320 – 7900	1.8 ± 0.2		3.0								10.[a].
7500 ± 200	1.5 ± 0.3		3.5 ± 0.5	−0.07	8.27	8.24	8.69				10.[b].
								6.6 ± 0.8			11.
7260 ± 200	1.83 ± 0.30										12.[a].
(7400)	(1.9)	7.94	4.5|5.7	−0.12	7.33					52.48	12.[b].
(7500)	1.2		3.0	+0.08 ± 0.10							13.
7460 ± 460									(1795)	25.5 ± 3.9	14.
7298 ± 150											15.
7500 ± 100	1.2 ± 0.2	8-9	2.8 ± 0.2	0.00							16.
(7500)	(1.5)	12.6									17.
7350	1.80	8	1.99-4.27 | 2.40-5.44	−0.3 ± 0.11						53	18.
7500 ± 200	1.5 ± 0.3		2.5 ± 0.5	0.06 ± 0.15	8.41 ± 0.10		8.63 ± 0.2				19.
7520 ± 460	<1.5							*(6.6)*			20.
(7350)	(1.80)	$12.8^{+24.95}_{-6.35}$	(3.25)	(−0.25)	(8.41)	(8.68)	(8.91)	7.22 ± 0.42	14573 ± 2268	74.39 ± 5.76	21.

1. Brown et al. (1974); 2. Code et al. (1976); 3. Blackwell & Shallis (1977); 4. Linsky & Ayres (1978); 5. Luck (1979); 6. Blackwell et al. (1980); 7. Desikachary & Hearnshaw (1982); 8. Boyarchuk & Lyubimkov (1983); 9. Lyubimkov & Boyarchuk (1984); 10. Luck & Lambert (1985); 11. di Benedetto & Rabbia (1987); 12. Russell & Bessell (1989); 13. Spite et al. (1989); 14. Volk & Cohen (1989); 15. McWilliam (1990); 16. Achmad et al. (1991); 17. El Eid (1994); 18. Gadun (1994); 19. Hill et al. (1995); 20. Smalley & Dworetsky (1995); 21. present results.

a luminosity of 12 000 $L_\odot$ would have been deduced, in close agreement with our results. Volk & Cohen (1989) found a luminosity of 1795 ± 71 $L_\odot$. This value was determined from the effective temperature, which was deduced directly from the literature values of angular diameter measurements, total-flux observations (from the literature) and the parallax from Hoffleit & Jaschek (1982). The parallax value mentioned by Hoffleit & Jaschek (1982) (π = 28 mas) is however a factor 2.68 higher than the value given by the Hipparcos catalogue. Using the Hipparcos' parallax would increase the stellar radius by the same amount – resulting in $R = 68\,R_\odot$ – and the luminosity by a factor 7.2 – giving $L \approx 13\,000\,L_\odot$, both values now being in good agreement with our deduced values.

3.3. β Leo: AOT01, speed 3, revolution 189

3.3.1. Some specific calibration details

β Leo is one of the few stars of our sample for which no speed-4 observation has been obtained. The signal-to-noise is therefore smaller than for the other *warm* stars. The shape of the spectrum in band 2 (after application of a standard calibration procedure) is very suspicious. A quick-look at the SPD (=Standard Processed Data, which gives the signal as a function of time) reveals immediately the origin of the problem. A photometric check is taken between the measurements with aperture 1 and aperture 2 and between the measurements with aperture 2 and aperture 3, i.e. just before the up scan of band 2A, and before the up scan of band 2C (Fig. 4). The calibration source is, however, much brighter than β Leo, resulting in a strong memory effect. Only the dark current before each measurement (at a certain aperture) has the same reset time as the measurement itself and could be used to subtract the dark current. Since the dark current before the measurement with aperture 3 (band 2C) is strongly affected by memory effects arising from the photometric check, the mean flux value of the dark current is higher than the flux values of the down scan beyond 9 μm. Therefore only the up scan of band 2C is used, and the fact is taken into account that memory effects are destroying the reliability of this up scan. In order to correct for this too high dark current, the data of band 2C are shifted upwards by 3.5 Jy (Table 3 in Paper II). The other factors used to combine the different sub-bands may also be found in Table 3 in Paper II.

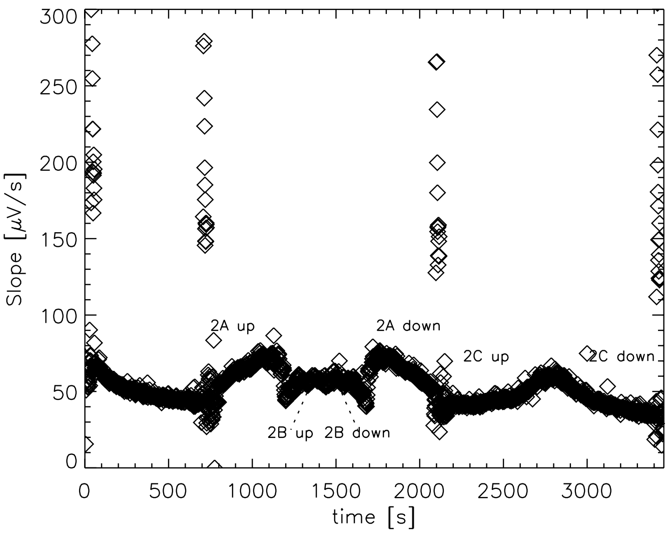

Fig. 4. The slope of detector 13 of band 2 of the AOT01 observation of β Leo (revolution 189) is plotted against time. The up and down scans of the different sub-bands are indicated. Photometric checks are taken between aperture 1 and aperture 2 and between aperture 2 and aperture 3.

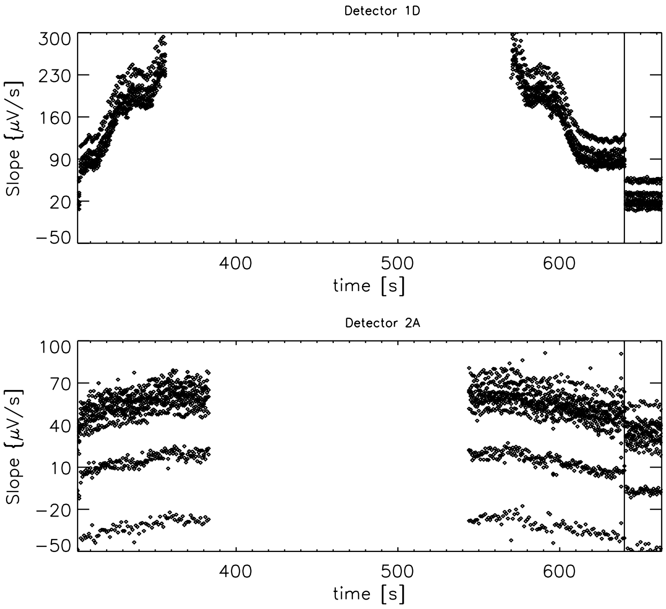

Fig. 5. The slope of the detectors in band 1D and band 2A of the AOT01 speed-1 observation of β Leo (revolution 040) are plotted against time. The signal jump is indicated by the vertical line.

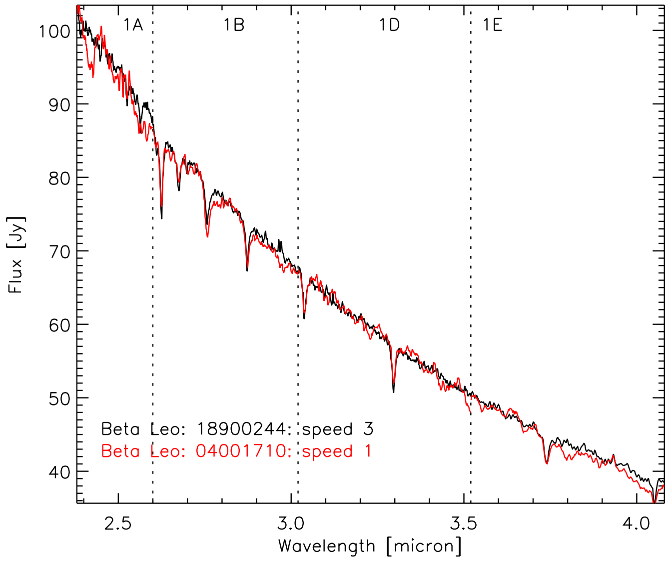

Fig. 6. Comparison between the AOT01 speed-3 observation of β Leo (revolution 189) and the speed-1 observation (revolution 040). The data of the speed-1 observation have been multiplied by a factor 1.05. A coloured version of this plot is available in the appendix as Fig. A.4.

3.3.2. Comparison with other AOT01 observations

β Leo has also been observed in revolution 040 during PV (Performance Verification) with the AOT01 speed-1 option. The pointing offsets were $dy = -0.737''$ and $dz = 0.913''$. Due to the triangular shape of the instrumental beam profile in the cross-dispersion direction of SWS, a pointing offset in the cross-dispersion direction causes a higher signal loss than in the dispersion-direction. For this observation, a photometric check was only taken before the up scan of band 2A and after the down scan of band 2C. So, only the up scan of band 2A can be affected by memory effects originating from the photometric check. The down scan of band 2A (and band 1D) displays however a signal jump 640 s after the start of the observation (Fig. 5). The origin of such signal jumps is at the moment unclear (Leech et al. 2002, p. 66). The jumps in bands 1 and 2 are similar to each other, but different from jumps in band 3. They can be negative or positive, and there seems to be a relation between the signal jump and a residual pulse effect after reset. It is recommended to adjust the baseline of the affected portion to the pre-jump baseline. For reason of safety, these data have been flagged as "no-data". In order to obtain a smooth spectrum, the data of the sub-bands 1A, 1B and 1E of this speed-1 observation have been multiplied by a factor 1.01.

The photometric flux level of this observation (revolution 040) is about 5% lower than the AOT01 speed-4 observation taken during revolution 189. A few differences between the two observed spectra are somewhat more pronounced, e.g. around 2.42 μm, 2.58 μm, 3.8 μm (see Fig. 6). Inaccuracies in the speed-1 observations – clearly visible from the comparison between up and down scan – originate from these discrepancies.

3.3.3. Comparison between the ISO-SWS spectrum and the synthetic spectrum (Fig. 7)

Good-quality published stellar parameters for β Leo were found in Holweger & Rentzsch-Holm (1995). These authors list as parameters: $T_{\rm eff}$ = 630 K, log g = 4.20. Using Strømgren photometry, Gardiner et al. (1999) obtained Fe/H] $\approx$ +0.2 dex. A microturbulent velocity of 2 km s^{-1} was assumed. With an angular diameter deduced from the ISO-SWS spectrum $\theta_{\rm d}$ = 1.47 ± 0.09 mas, one obtains R = 1.75 ± 0.11 $R_\odot$, $M_{\rm g}$ = 1.78 ± 1.04 $M_\odot$ and L = 15 ± 3 $L_\odot$. The corresponding deviation estimating parameters are $\beta_{\rm 1A}$ = 0.060, $\beta_{\rm 1B}$ = 0.028, $\beta_{\rm 1D}$ = 0.087, $\beta_{\rm 1E}$ = 0.038.

The large β-values for β Leo are not very surprising. One first of all has to take into account the problems with the hydrogen lines, which dominate the spectrum. Secondly, for band 1A, there is also a large discrepancy at the wavelengths were the H5-23 and H5-22 lines emerge at the beginning of this band. A problem with the RSRF is at the origin of this discrepancy Paper II. The large $\beta_{\rm 1D}$-value is arising from the problems nearby the Humphreys ionisation edge Paper II. The lower signal/noise ratio in a AOT01 speed-3 observation compared to the other observations also contributes to larger β-values.

3.3.4. Comparison with other published stellar parameters

– Assumed parameters:
From the detailed investigation by Smalley & Dworetsky (1993), one may conclude that atmospheric parameters derived from photometry, spectrophotometry and from Hβ and Hγ profiles all agree quite well, provided that adequate opacities and metallicities are used. Especially the values of the effective temperature and gravity should be

Table 4. See caption of Table 2, but now for β Leo.

$T_{\rm eff}$	$\log g$	M	ξ_t	[Fe/H]	ε(C)	ε(N)	ε(O)	θ_d	L	R	Ref.
								1.33 ± 0.10			1.
8850 ± 340								(*1.33*)			2.
								1.32		1.73	3.
8660										1.73	4[a].
8660										1.68	4[b].
8600	4.2										5.
9590 ± 460	4.27 ± 0.15	2.3						1.39 ± 0.03	25.1 ± 7.2	1.82 ± 0.18	6.
8850											7.
8500	4.20			0.00							8[a].
8640	4.37			0.50							8[b].
8310	4.20			0.00							8[c].
8260	4.37			0.50							8[d].
8630	4.21										9.
8870 ± 350	4.00 ± 0.25							(*1.40*)			10[a].
8870 ± 350	4.10 ± 0.30							(*1.33*)			10[b].
8720 ± 300											11.
8857 ± 185	4.0							1.374 ± 0.033			12.
(8870)	(4.10)			0.20							13.
(8630)	(4.20)	1.78 ± 0.46	(2.0)	(0.00)	(8.76)	(8.25)	(9.13)	1.47 ± 0.09	15 ± 2	1.75 ± 0.11	14.

1. Brown et al. (1974); 2. Code et al. (1976); 3. Moon (1985); 4. Moon & Dworetsky (1985); 5. Lester et al. (1986); 6. Malagnini & Morossi (1990); 7. Napiwotzki et al. (1993); 8. Smalley & Dworetsky (1993); 9. Holweger & Rentzsch-Holm (1995); 10. Smalley & Dworetsky (1995); 11. Sokolov (1995); 12. Malagnini & Morossi (1997); 13. Gardiner et al. (1999); 14. present results.

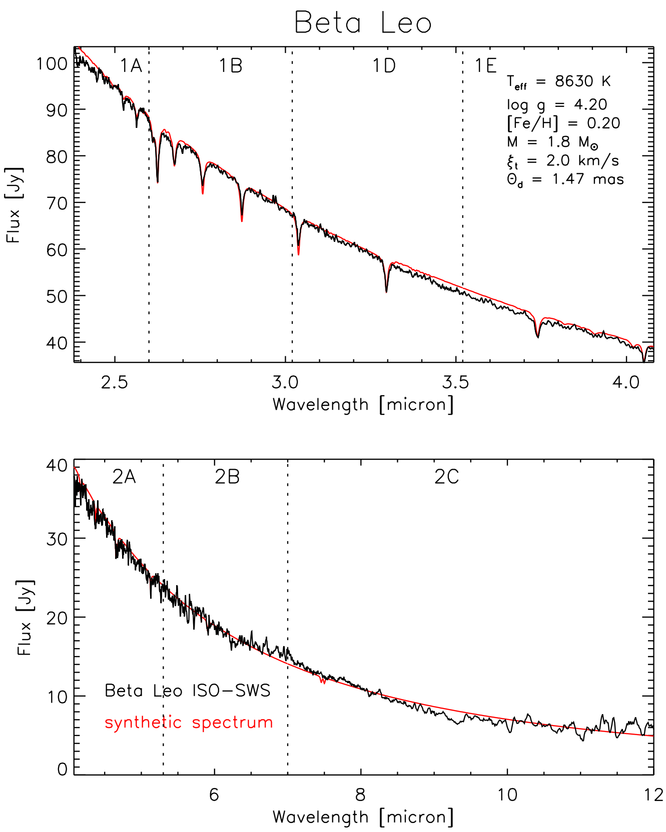

Fig. 7. Comparison between band 1 and band 2 of the ISO-SWS data of β Leo (black) and the synthetic spectrum (grey) with stellar parameters $T_{\rm eff}$ = 8630 K, $\log g$ = 4.20, M = 1.8 $M_\odot$, [Fe/H] = 0.20, ξ_t = 2.0 km s^{-1} and θ_d = 1.47 mas. A coloured version of this plot is available in the appendix as Fig. A.5.

very reliable when determined from photometry, and they should not be significantly affected by uncertainties in the metallicity (Smalley & Dworetsky 1993). From the research of Gardiner et al. (1999), one may however conclude that the determination of the effective temperature and the gravity for this star from Balmer line profiles (as done e.g. by Smalley & Dworetsky 1995) seems to be rather uncertain, because β Leo is located close to the maximum of the Balmer line width. Therefore, the values found by Holweger & Rentzsch-Holm (1995) – who have used Strömgren photometry – were taken as stellar parameters for the theoretical model and corresponding synthetic spectrum. Since Gardiner et al. (1999) estimated β Leo to be slightly overabundant ([Fe/H] $\approx$ +0.2 dex) from Strömgren photometry, this value was assumed for the metallicity. For the microturbulent velocity a value of 2 km s^{-1} was assumed.

– Deduced parameters:
  Malagnini & Morossi (1990, 1997) have used a flux-fitting method which determines simultaneously the effective temperature and the angular diameter. Their obtained values agree well with the angular diameter deduced from the ISO-SWS spectrum. The small differences in the luminosity and radius values mentioned by Malagnini & Morossi (1990) are partly due to the use of the parallax value of Hoffleit & Jaschek (1982), which is a factor 1.1 lower than the Hipparcos' parallax. When we then compare our gravity-inferred mass with the mass estimated from evolutionary tracks by Malagnini & Morossi (1990), we see that our deduced value is somewhat lower than their quoted value. Using $\log T_{\rm eff}$ = 3.936 and $\log L$ = 1.176 ± 0.058, we estimated from the evolutionary tracks of Girardi et al. (2000) a mass of 1.9 $M_\odot$, which is thus somewhat closer to the value of 2.3 $M_\odot$, given by Malagnini & Morossi (1990).

3.4. Sirius: AOT01, speed 4, revolution 689

3.4.1. Some specific calibration details

The speed-4 observation of Sirius only suffered from very small pointing errors. Bands 1A and 1B were shifted upwards by 1%, band 1E was shifted downwards by 0.5%.

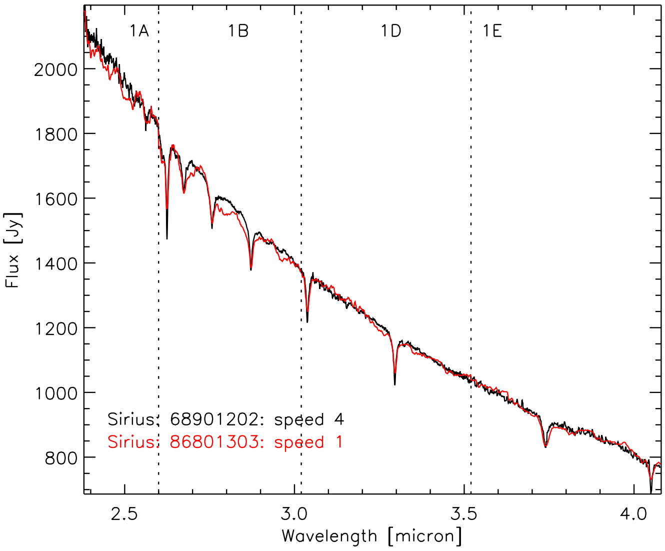

Fig. 8. Comparison between the AOT01 speed-4 observation of α CMa (revolution 689) and the speed-1 observation (revolution 868). The data of the speed-1 observation have been multiplied by a factor 1.12. A coloured version of this plot is available in the appendix as Fig. A.6.

3.4.2. Comparison with other AOT01 observations

At the end of the ISO mission – during revolution 868 – Sirius was once more observed using the AOT01 mode, but now with a higher speed, resulting in a lower resolution and a lower signal-to-noise ratio. The pointing offsets were negligible. Only the data of band 1A were divided by a factor 1.01 to optimise the match between the different sub-bands. The absolute-flux levels differ however by 12% (Fig. 8). With a quoted absolute-flux accuracy of 10% and the template of Cohen (Cohen et al. 1992a) being in absolute-flux level in between these two observations this difference is not worrying.

Taking the lower signal-to-noise ratio of the speed-1 observation into account, the features of the two observational spectra of Sirius do agree well.

3.4.3. Comparison between the ISO-SWS spectrum and the synthetic spectrum (Fig. 9)

For Sirius the effective temperature, the gravity and the metallicity were taken from Bell & Dreiling (1981), while the microturbulence and the abundances of C, N and O are the values found by Lambert et al. (1982) who have used the model parameters found by Bell & Dreiling (1981). The adopted stellar parameters for Sirius are thus $T_{\rm eff}$ = 10150 K, $\log g$ = 4.30, $\xi_{\rm t}$ = 2.0 km s^{-1}, [Fe/H] = 0.50, ε(C) = 7.97, ε(N) = 8.15, ε(O) = 8.55, π = 379.21 ± 1.58 mas, resulting in $\theta_{\rm d}$ = 6.17 ± 0.38 mas, $R = 1.75 \pm 0.11\,R_{\odot}$, $M_{\rm g} = 2.22 \pm 1.06\,M_{\odot}$ and $L = 29 \pm 6\,L_{\odot}$. Using these parameters, the deviation estimating parameters β from the Kolmogorov-Smirnov statistics are $\beta_{\rm 1A} = 0.041, \beta_{\rm 1B} = 0.017, \beta_{\rm 1D} = 0.098$ and $\beta_{\rm 1E} = 0.027$.

Sirius is the star in our sample with the highest gravity. So, it is not surprising that the synthetic spectrum deviates largely from the observed spectrum in band 1D, where the Humphreys

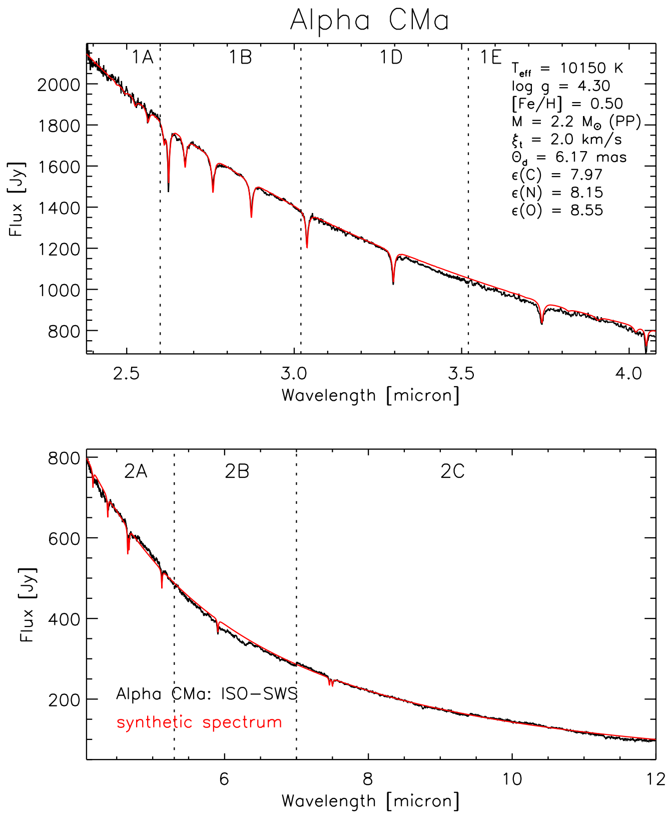

Fig. 9. Comparison between band 1 and band 2 of the ISO-SWS data of α CMa (black) and the synthetic spectrum (grey) with stellar parameters $T_{\rm eff}$ = 10 150 K, $\log g$ = 4.30, $M = 2.2\,M_{\odot}$, [Fe/H] = 0.50, $\xi_{\rm t}$ = 2.0 km s^{-1}, ε(C) = 7.97, ε(N) = 8.15, ε(O) = 8.55 and $\theta_{\rm d}$ = 6.17 mas. A coloured version of this plot is available in the appendix as Fig. A.7.

lines determine the spectral signature. The pronounced discrepancy seen around 6 μm is a consequence of the use of an inaccurate model for the memory-effect correction in the OLP6.0 calibration of the ISO-SWS data. Consequently the relative spectral response functions are still not well determined in band 2.

3.4.4. Comparison with other published stellar parameters

– Assumed parameters:
Several authors determined the effective temperature and the surface gravity for Sirius by using *uvbyβ* photometry and the grids of Moon & Dworetsky (1985) (e.g., Lemke 1990; Hill & Landstreet 1993; Hui-Bon-Hoa et al. 1997). The values of the effective temperature obtained in that way are in between the values derived from the IRFM (e.g., Blackwell et al. 1980) and the values derived from comparing observed and theoretical fluxes (e.g., Bell & Dreiling 1981), with the IRFM-results being the lowest ones. The derived values for the gravity from the Balmer line profile and from photometric data are in good agreement, and more or less the same abundance pattern is derived by different authors. The microturbulence and C, N and O abundance

Table 5. See caption of Table 2, but now for Sirius.

$T_{\rm eff}$	$\log g$	M	$\xi_{\rm t}$	[Fe/H]	ε(C)	ε(N)	ε(O)	$\theta_{\rm d}$	L	R	Ref.
9697								6.20			1.
(9440)	(4.33)	(2.20)							(23.4)	(1.68)	2.
10150 ± 400	4.30 ± 0.20	(2.1)		0.50 ± 0.30							3.
(10 150)	(4.30 ± 0.20)		2.0 ± 0.5	0.60 ± 0.30	7.97 ± 0.15	8.15 ± 0.15	8.55 ± 0.12				4.
								5.89		1.675	5.
9900	4.32										6.
(10 000)	(4.30)		2.0	0.50							7.
10100									(26.75)	1.69 ± 0.05	8.
9900	4.30		2.0		7.85 ± 0.06						9.
9870	4.32		1.7 ± 0.2	0.28	7.82	> 8.20					10.
9940 ± 210	(4.33)	(2.20)									11[a].
9940 ± 210	4.20 ± 0.15	(2.20)									11[b].
9940 ± 210	4.3 ± 0.5	(2.20)									11[c].
9870 ± 200	4.40 ± 0.14		2.0	0.49 ± 0.29							12.
9900	4.30		2.0	0.64	8.03 ± 0.54						13.
9945 ± 122								*5.92 ± 0.09*			14[a].
9943								*5.86*			14[b].
(9880)	4.40 ± 0.20		1.85 ± 0.30	0.50	7.64 ± 0.06	8.04 ± 0.15	8.63 ± 0.05				15.
(10 150)	(4.30)	2.22 ± 1.06	(2.0)	(0.50)	(7.97)	(8.15)	(8.55)	6.17 ± 0.38	29 ± 6	1.75 ± 0.11	16.

1. Blackwell et al. (1980); 2. Popper (1980); 3. Bell & Dreiling (1981); 4. Lambert et al. (1982); 5. Moon (1985); 6. Moon & Dworetsky (1985); 7. Sadakane & Ueta (1989); 8. Volk & Cohen (1989); 9. Lemke (1990); 10. Hill & Landstreet (1993); 11. Smalley & Dworetsky (1995); 12. Hui-Bon-Hoa et al. (1997); 13. Rentzsch-Holm (1997); 14. di Benedetto (1998); 15. Qiu et al. (2001); 16. present results.

deduced by Lambert et al. (1982) were assumed as input parameters, who have taken $T_{\rm eff}$, $\log g$ and [Fe/H] from Bell & Dreiling (1981) as model parameters.

– Deduced parameters:
The only indirect measurement of the angular diameter available is from IRFM. Our derived angular diameter of $\theta_{\rm d}$ = 6.17 ± 0.38 mas corresponds with the value of Blackwell et al. (1980). Contrary to the target α Car, a good agreement is found for the luminosity and radius values of Sirius between our deduced values and the ones of Volk & Cohen (1989). The reason is situated in the Hipparcos' parallax now being almost the same as the parallax of Hoffleit & Jaschek (1982) (π = 378 mas), used to determine R and L from $\theta_{\rm d}$. Moon (1985) used a quite different method, based on a new relation between the visual surface brightness F_v and the $(b-y)_0$ colour index of $uvby\beta$ photometry (see the appendix available at `http://www.ster.kuleuven.ac.be/~leen/artikels/ISO3/appendix.ps`). His quoted value lies within the error bars of our deduced value.
Not only for Sirius, but also for other warm stars in the sample, we note a large error bar on the derived mass $M_{\rm g}$, which mainly depends on the error in the gravity. This demonstrates that other methods for mass determination (e.g. from data of eclipsing and visual binaries) are far more useful than the underlying method for the $M_{\rm g}$ determination (from the gravity and the radius).

3.5. Vega: AOT01, speed 3, revolution 178

3.5.1. Some specific calibration details

This speed-3 observation of Vega in revolution 178 had some problems with the pointing: dy = −0.608″ and dz = −1.179″. Switching then to a larger aperture between band 1B and band 1D results in a flux-jump, which is clearly visible in the factors used to shift the different sub-bands. In order to have a smooth spectrum, we had to multiply the data of bands 1A and 1B by a factor 1.06 (see Table 3 in Paper II).

3.5.2. Comparison between the ISO-SWS spectrum and the synthetic spectrum (Fig. 10)

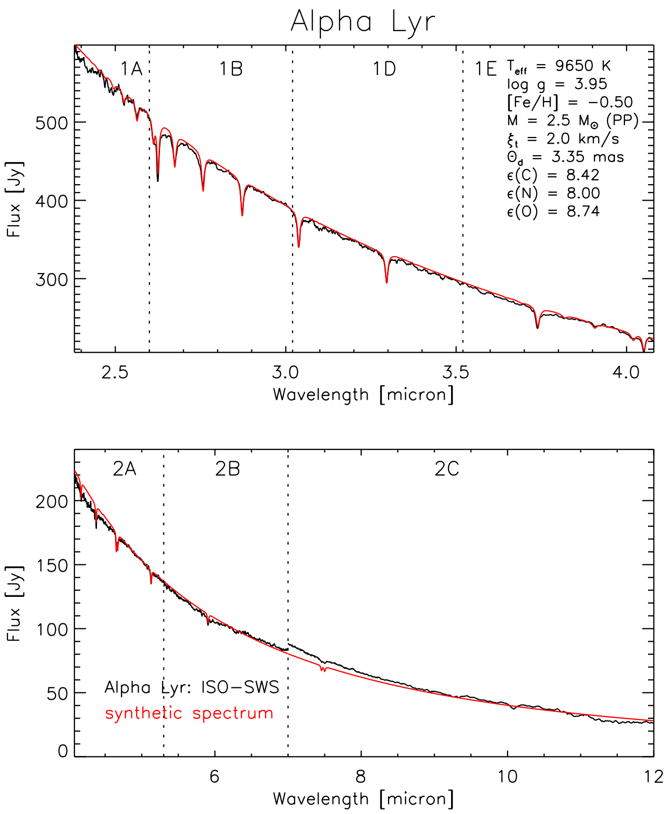

Fig. 10. Comparison between band 1 and band 2 of the ISO-SWS data of α Lyr (black) and the synthetic spectrum (grey) with stellar parameters $T_{\rm eff}$ = 9650 K, $\log g$ = 3.95, M = 2.5 $M_\odot$, [Fe/H] = −0.50, $\xi_{\rm t}$ = 2.0 km s^{-1}, ε(C) = 8.42, ε(N) = 8.00, ε(O) = 8.74 and $\theta_{\rm d}$ = 3.35 mas. A coloured version of this plot is available in the appendix as Fig. A.8.

Table 6. See caption of Table 2, but now for Vega.

$T_{\rm eff}$	$\log g$	M	$\xi_{\rm t}$	[Fe/H]	ε(C)	ε(N)	ε(O)	$\theta_{\rm d}$	L	R	Ref.
9468								3.35			1.
9650	3.90 ± 0.20	(2.0)		−0.41 ± 0.30				*3.24 ± 0.07*		2.83	2.
(9660)	(3.94)		2.0	−0.60							3.
(9650)	(3.90)		2.0 ± 0.5	−0.40 ± 0.30	8.57 ± 0.15	7.93 ± 0.15	8.82 ± 0.12				4.
										2.588	5[a].
										2.234	5[b].
9500	3.90										6.
(9500)	(3.90)		2.0	−0.55 ± 0.10							7.
									(62.66)	2.83 ± 0.13	8.
(9400)	(3.95)		0.6	−0.56 ± 0.15	8.19						9.
9500	3.90				8.49						10.
(9650)	(3.95)		(2.0)	−0.53 ± 0.15	8.42 ± 0.15	8.00 ± 0.15	8.74 ± 0.15				11.
9560	4.05		2.0 ± 0.2	−0.54	8.47	>8.40					12.
9600											13.
9450	4.00		(2.0)	−0.56 ± 0.05							14.
9550 ± 50	3.95 ± 0.05		(2.0)	−0.50							15.
9600 ± 180	4.00 ± 0.10										16[a].
9600 ± 180	3.80 ± 0.30										16[b].
9830 ± 320											17[a].
9660											17[b].
9660 ± 140								*3.24 ± 0.07*			18[a].
9469								*3.20*			18[b].
9553 ± 111								*3.28 ± 0.01*			19.
(9430)	3.95 ± 0.20		1.50 ± 0.30	−0.57	8.46 ± 0.13	8.00 ± 0.02	9.01 ± 0.14				20.
(9650)	(3.95)	2.54 ± 1.21	(2.0)	(−0.50)	(8.42)	(8.00)	(8.74)	3.35 ± 0.20	61 ± 9	2.79 ± 0.17	21.

1. Blackwell et al. (1980); 2. Dreiling & Bell (1980); 3. Sadakane & Nishimura (1981); 4. Lambert et al. (1982); 5. Moon (1985); 6. Moon & Dworetsky (1985); 7. Gigas (1986); 8. Volk & Cohen (1989); 9. Adelman & Gulliver (1990); 10. Lemke (1990); 11. Venn & Lambert (1990); 12. Hill & Landstreet (1993); 13. Napiwotzki et al. (1993); 14. Smith & Dworetsky (1993); 15. Castelli & Kurucz (1994); 16. Smalley & Dworetsky (1995); 17. Sokolov (1995); 18. di Benedetto (1998); 19. Ciardi et al. (2001); 20. Qiu et al. (2001); 21. present results.

As will be discussed in Sect. 3.5.3, the following stellar parameters were adopted for Vega: $T_{\rm eff}$ = 9650 K, $\log g$ = 3.95, $\xi_{\rm t}$ = 2.0 km s^{-1}, [Fe/H] = −0.50, ε(C) = 8.42, ε(N) = 8.00, ε(O) = 8.74. From the ISO-SWS spectrum of Vega, an angular diameter of 3.35 ± 0.20 mas was deduced, with then yields a stellar radius of 2.79 ± 0.17 $R_\odot$, a gravity-inferred mass of 2.54 ± 1.21 $M_\odot$ and a stellar luminosity of 61 ± 9 $L_\odot$. Both the synthetic spectrum based on these parameters and the ISO-SWS spectrum of Vega are displayed in Fig. 10. The corresponding β-values are $\beta_{\rm 1A} = 0.057, \beta_{\rm 1B} = 0.046, \beta_{\rm 1D} = 0.010$, $\beta_{\rm 1E} = 0.041$.

In spite of the lower signal-to-noise and lower resolution of the ISO-SWS observation, good β-values are obtained. One indeed would not expect such a low β-value in band 1D, the wavelength-range in which the hydrogen Humphreys lines are absorbing. The reason for this is twofold: first of all, Vega has the lowest gravity in our sample of main-sequence stars, resulting in a smaller pressure-broadening and thus in smaller hydrogen lines. Consequently, the discrepancy with the synthetic predictions, which underestimate the strength of the Humphreys lines, is not as pronounced as for the other main-sequence stars in our sample. Secondly, Vega has been observed by using the AOT01 speed-3 option and we have already pointed out the small – but visible in the spectrum – mispointing for this observation. The larger noise inherent to this observation can therefore partly camouflage the problem with the theoretical computation of the hydrogen Humphreys lines. Our statistical test will not report this problem, since the Kolmogorov-Smirnov test is a *global* goodness-of-fit test and fitting by eye was still necessary to detect this kind of problems. A new statistical approach in which a *global* and *local* goodness-of-fit test are combined is therefore now under development.

3.5.3. Comparison with other published stellar parameters

The bright star Vega has been studied extensively in recent years because it serves as the primary standard star for photoelectric spectrophotometry. Since so many publications are available for this star – as well as for Sirius – we only have quoted the main publications in the last two decades.

- Assumed parameters:
  Inspecting Table 6, we can see that the published values for the different parameters all do agree well. As for Sirius, the temperature values derived from IRFM are somewhat lower than the other published values (see also the remark made by Napiwotzki et al. (1993), who quoted that the IRFM temperatures are too low by 1.6–2.8% for main-sequence stars). A detailed study of Vega was made by Dreiling & Bell (1980). From this study Venn & Lambert (1990) have adopted the effective temperature ($T_{\rm eff}$ = 9650 K) and the gravity ($\log g$ = 3.95). Using the microturbulent velocity found by Lambert et al. (1982) ($\xi_{\rm t}$ = 2.0 km s^{-1}), Venn & Lambert (1990) have determined the chemical composition for Vega. Using the solar metallicity obtained from meteoritic data, ε(Fe) = 7.51, as a reference value, their abundances for carbon, nitrogen, oxygen and iron were respectively: ε(C) = 8.42 ± 0.15, ε(N) = 8.00 ± 0.15, ε(O) = 8.74 ± 0.15 and [Fe/H] = −0.53 ± 0.15.
- Deduced parameters:
  Our angular diameter derived from the ISO-SWS spectrum corresponds to the IRFM value from Blackwell et al. (1980). The same note as made in Sect. 3.4.4 concerning the luminosity and radius values mentioned by Volk & Cohen (1989) can be made: since the parallax value mentioned by Hoffleit & Jaschek (1982) (π = 133 mas) only

differs with the Hipparcos' value by a factor 1.03, the values for R and L are in close agreement. This can also be said for the radius value given by Dreiling & Bell (1980), who too have used the parallax of Hoffleit & Jaschek (1982). The new relation established by Moon (1985) results in stellar radius values which are somewhat lower than our deduced value and the values mentioned by Moon (1985) and Volk & Cohen (1989).

4. Conclusion

The five warmest stars in a sample of 16 stars – used for the calibration of the detectors of ISO-SWS – have been discussed spectroscopically. The absence of molecular features and the presence of atomic features whose oscillator strengths are not well-known rendered the determination of the effective temperature, gravity, microturbulent velocity, metallicity and the abundance of C, N, and O from the ISO-SWS data unfeasible. Good-quality published values were then used for the computation of the synthetic spectra. In general, no more discrepancies than the ones reported in Paper II have been detected. A comparison with other – lower resolution – ISO-SWS data revealed a rather good relative agreement (∼2%), but the absolute flux-level and so the deduced angular diameter could differ by up to 16%. Nevertheless, the angular diameter, luminosity and stellar radius deduced from the ISO-SWS data are in good agreement with other published values deduced from other data and/or methods.

Since this research has shown clearly that the available oscillator strengths of atomic transitions in the infrared are at the moment still very inaccurate, one of us (J. S.) has worked on a new atomic linelist by deducing new oscillator strengths from the high-resolution ATMOS spectrum of the Sun (625–4800 cm^{-1}) (Sauval 2002). This new atomic linelist will be presented in Paper V of this series.

Acknowledgements. LD acknowledges support from the Science Foundation of Flanders. This research has made use of the SIMBAD database, operated at CDS, Strasbourg, France and of the VALD database, operated at Vienna, Austria. It is a pleasure to thank the referees, J. Hron and F. Kupka, for their careful reading of the manuscript and for their valuable suggestions.

References

Abia, C., Rebolo, R., Beckman, J. E., & Crivellari, L. 1988, A&A, 206, 100
Achmad, L., de Jager, C., & Nieuwenhuijzen, H. 1991, A&A, 249, 192
Adelman, S. J., & Gulliver, A. F. 1990, ApJ, 348, 712
Balona, L. A. 1984, MNRAS, 211, 973
Becker, S. A. 1981, ApJS, 45, 475
Bell, R. A., & Dreiling, L. A. 1981, ApJ, 248, 1031
Bessell, M. S., Castelli, F., & Plez, B. 1998, A&A, 333, 231
Blackwell, D. E., Petford, A. D., & Shallis, M. J. 1980, A&A, 82, 249
Blackwell, D. E., & Shallis, M. J. 1977, MNRAS, 180, 177
Boyarchuk, A. A., & Lyubimkov, L. S. 1983, Astrophys., 18, 228
Brown, J. A., Tomkin, J., & Lambert, D. L. 1983, ApJ, 265, L93
Brown, R. H., Davis, J., & Allen, L. R. 1974, MNRAS, 167, 121
Castelli, F., & Kurucz, R. L. 1994, A&A, 281, 817
Cayrel, R., Cayrel de Strobel, G., & Campbell, B. 1985, A&A, 146, 249
Chmielewski, Y., Friel, E., Cayrel de Strobel, G., & Bentolila, C. 1992, A&A, 263, 219
Ciardi, D. R., van Belle, G. T., Akeson, R. L., et al. 2001, ApJ, 559, 1147
Claret, A., & Gimenez, A. 1995, A&AS, 114, 549
Code, A. D., Bless, R. C., Davis, J., & Brown, R. H. 1976, ApJ, 203, 417
Cohen, M., Walker, R. G., Barlow, M. J., & Deacon, J. R. 1992a, AJ, 104, 1650
Cohen, M., Walker, R. G., & Witteborn, F. C. 1992b, AJ, 104, 2030
Cohen, M., Witteborn, F. C., Bregman, J. D., et al. 1996a, AJ, 112, 241
Cohen, M., Witteborn, F. C., Carbon, D. F., et al. 1996b, AJ, 112, 2274
Cohen, M., Witteborn, F. C., Walker, R. G., Bregman, J. D., & Wooden, D. H. 1995, AJ, 110, 275
Decin, L. 2000, Ph.D. Thesis, University of Leuven
Decin, L., Vandenbussche, B., Waelkens, C., et al. 2003, A&A, 400, 679 (Paper II)
Decin, L., Waelkens, C., Eriksson, K., et al. 2000, A&A, 364, 137
Demarque, P., Guenther, D. B., & van Altena, W. F. 1986, ApJ, 300, 773
Desikachary, K., & Hearnshaw, J. B. 1982, MNRAS, 201, 707
di Benedetto, G. P. 1998, A&A, 339, 858
di Benedetto, G. P., & Rabbia, Y. 1987, A&A, 188, 114
Dreiling, L. A., & Bell, R. A. 1980, ApJ, 241, 736
Edvardsson, B. 1988, A&A, 190, 148
El Eid, M. F. 1994, A&A, 285, 915
Engelke, C. W. 1992, AJ, 104, 1248
England, M. N. 1980, MNRAS, 191, 23
Feuchtgruber, H. 1998, Status of AOT01 AOT band order ratios and related data (ISO-SWS online documentation)
Flannery, B. P., & Ayres, T. R. 1978, ApJ, 221, 175
Fracassini, M., Pasinetti-Fracassini, L. E., Pastori, L., & Pironi, R. 1988, Bulletin d'Information du Centre de Donnees Stellaires, 35, 121
Furenlid, I., & Meylan, T. 1990, ApJ, 350, 827
Gadun, A. S. 1994, Astronomische Nachrichten, 315, 413
Gardiner, R. B., Kupka, F., & Smalley, B. 1999, A&A, 347, 876
Geller, M. 1992, A High-Resolution Atlas of the Infrared Spectrum of the Sun and Earth Atmosphere from Space, vol. III, Key to Identification of Solar Features (Washington, D.C.: NASA, Scientific and Technical Information Division)
Gigas, D. 1986, A&A, 165, 170
Girardi, L., Bressan, A., Bertelli, G., & Chiosi, C. 2000, A&AS, 141, 371
Gliese, W. 1969, Veröffentlichungen des Astronomishen Rechen-Instituts Heidelberg, 22, 1
Gunson, M. R., Abbas, M. M., Abrams, M. C., et al. 1996, Geophys. Res. Lett., 23, 2333
Gustafsson, B., Bell, R. A., Eriksson, K., & Nordlund, Å. 1975, A&A, 42, 407
Harris, M. J., & Lambert, D. L. 1984, ApJ, 285, 674
Hill, G. M., & Landstreet, J. D. 1993, A&A, 276, 142
Hill, V., Andrievsky, S., & Spite, M. 1995, A&A, 293, 347
Hirata, R., & Horaguchi, T. 1995, Atomic spectral line list `http://cdsweb.u-strasbg.fr/htbin/Cat?VI/69`
Hoffleit, D., & Jaschek, C. 1982, The Bright Star Catalogue (4th edition) (The Bright Star Catalogue (New Haven: Yale University Observatory)
Holweger, H., & Rentzsch-Holm, I. 1995, A&A, 303, 819
Hui-Bon-Hoa, A., Burkhart, C., & Alecian, G. 1997, A&A, 323, 901

Johnson, H. L., Iriarte, B., Mitchell, R. I., & Wisniewskj, W. Z. 1966, Communications of the Lunar and Planetary Laboratory, 4, 99
Kamper, K. W., & Wesselink, A. J. 1978, AJ, 83, 1653
Kurucz, R. 1993, ATLAS9 Stellar Atmosphere Programs and 2 km/s grid, Kurucz CD-ROM No. 13 (Cambridge, MA: Smithsonian Astrophysical Observatory)
Kurucz, R. L. 1970, SAO Special Report, 308
Kurucz, R. L. 1979, ApJS, 40, 1
Kurucz, R. L. 1991, in Stellar Atmospheres: Beyond Classical Models, Proc. of the Advanced Research Workshop., 441
Kurucz, R. L., & Furenlid, I. 1979, Smithsonian Astrophys. Obs. Spec. Rept., 387
Lambert, D. L., Roby, S. W., & Bell, R. A. 1982, ApJ, 254, 663
Lane, M. C., & Lester, J. B. 1984, ApJ, 281, 723
Leech, K., Kester, D., Shipman, R., et al. 2002, in The ISO Handbook, vol. V, SWS – The Short Wavelength Spectrometer, ed. K. Leech
Lemke, M. 1990, A&A, 240, 331
Lester, J. B., Gray, R. O., & Kurucz, R. L. 1986, ApJS, 61, 509
Linsky, J. L., & Ayres, T. R. 1978, ApJ, 220, 619
Luck, R. E. 1979, ApJ, 232, 797
Luck, R. E., & Lambert, D. L. 1985, ApJ, 298, 782
Lyubimkov, L. S., & Boyarchuk, A. A. 1984, Astrophys., 19, 385
Malagnini, M. L., & Morossi, C. 1990, A&AS, 85, 1015
Malagnini, M. L., & Morossi, C. 1997, A&A, 326, 736
Malagnini, M. L., Morossi, C., Rossi, L., & Kurucz, R. L. 1986, A&A, 162, 140
McWilliam, A. 1990, ApJS, 74, 1075
Moon, T. 1985, Ap&SS, 117, 261
Moon, T. T., & Dworetsky, M. M. 1985, MNRAS, 217, 305
Napiwotzki, R., Schönberner, D., & Wenske, V. 1993, A&A, 268, 653
Neuforge-Verheecke, C., & Magain, P. 1997, A&A, 328, 261
Plez, B., Brett, J. M., & Nordlund, Å. 1992, A&A, 256, 551
Plez, B., Smith, V. V., & Lambert, D. L. 1993, ApJ, 418, 812
Popper, D. M. 1980, ARA&A, 18, 115
Popper, D. M. 1993, ApJ, 404, L67
Pottasch, E. M., Butcher, H. R., & van Hoesel, F. H. J. 1992, A&A, 264, 138
Pourbaix, D., Neuforge-Verheecke, C., & Noels, A. 1999, A&A, 344, 172
Qiu, H., Zhao, G., Chen, Y. Q., & Li, Z. W. 2001, A&A, 548, 953
Relyea, L. J., & Kurucz, R. L. 1978, ApJS, 37, 45
Rentzsch-Holm, I. 1997, A&A, 317, 178
Russell, S. C., & Bessell, M. S. 1989, ApJS, 70, 865
Sadakane, K., & Nishimura, M. 1981, PASJ, 33, 189
Sadakane, K., & Ueta, M. 1989, PASJ, 41, 279
Sauval, A. J. 2002, Data file of IR solar atomic lines (unpublished results)
Smalley, B., & Dworetsky, M. M. 1993, A&A, 271, 515
Smalley, B., & Dworetsky, M. M. 1995, A&A, 293, 446
Smalley, B., & Kupka, F. 1997, A&A, 328, 349
Smith, G., Edvardsson, B., & Frisk, U. 1986, A&A, 165, 126
Smith, K. C., & Dworetsky, M. M. 1993, A&A, 274, 335
Smith, V. V., & Lambert, D. L. 1985, ApJ, 294, 326
Smith, V. V., & Lambert, D. L. 1986, ApJ, 311, 843
Soderblom, D. R. 1986, A&A, 158, 273
Sokolov, N. A. 1995, A&AS, 110, 553
Spite, F., Spite, M., & Francois, P. 1989, A&A, 210, 25
Trimble, V., & Bell, R. A. 1981, QJRAS, 22, 361
Venn, K. A., & Lambert, D. L. 1990, ApJ, 363, 234
Volk, K., & Cohen, M. 1989, AJ, 98, 1918
Witteborn, F. C., Cohen, M., Bregman, J. D., et al. 1999, AJ, 117, 2552